

Tunneling escape time of electrons from the quasibound Stark localized states in ultrathin barrier GaAs/AlAs superlattices

K. Fujiwara, K. Kawashima, and T. Imanishi
Kyushu Institute of Technology, Tobata, Kitakyushu 804, Japan
 (Received 1 July 1996)

Band-edge optical absorption spectra in two series of monoperoiodic GaAs/AlAs superlattice diodes are investigated as a function of bias voltage by low-temperature photocurrent spectroscopy. In the superlattices the well width is fixed at 11 or 22 monolayers (ML) and only the ultrathin barrier thickness is varied between 2 and 6 ML. In the limit of high electric field conditions where the fundamental Stark ladder transition dominates, the linewidth of the heavy-hole excitonic peak is found to increase systematically with decreasing the barrier thickness. That is, the linewidth for the superlattice with thinner barriers is broader than that with the thick barrier superlattice, which is basically determined by the usual inhomogeneous broadening. This enhancement of the spectral linewidth by more than 10 meV is due to a lifetime broadening of the quasibound Stark localized states. This resonance energy broadening due to the rapid tunneling escape of electrons is used to determine the tunneling time by the uncertainty principle. The tunneling escape time thus determined as a function of barrier thickness shows good agreement with values deduced from the confined electron level broadening for the biased double-barrier quantum-well structures based on simple transfer matrix calculations. [S0163-1829(96)09348-4]

I. INTRODUCTION

Recently, external electric field effects (Stark effects) in semiconductor superlattices (SL's), i.e., so-called Wannier-Stark localization, have been receiving a great deal of attention.¹⁻⁹ The existence of equally spaced energy levels, Stark ladders, and Bloch oscillations, which were predicted in the late 1950s,¹ has actually been demonstrated. Moreover, these effects are also found to be very useful for applications to new optoelectronic devices.^{10,11}

Under the high axial electric field (F) applied along the superlattice-growth z direction, the resonant coupling between the individual quantum wells (QW's) can significantly be weakened or even destroyed because of the energy misalignment by $neFD$ between the neighboring wells separated by multiples (n) of the SL period D (Stark effects). As a result, the wave functions associated with the Stark ladders are partially localized, with each eigenstate being peaked in the individual wells, but with its amplitude substantially decreasing into a few neighboring wells. When an extremely high field is applied, the eigenstate is completely localized within each well and the discrete QW eigenenergy levels can be recovered. In fact, the Stark localized states are definitely observed in numerous optical absorption spectra involved with the quasi-two-dimensional excitonic effects.³⁻⁶ However, we should note that the Stark localized states are no longer the same as the usual QW subband states originally localized within the flat potential well since the electrostatic term is added in the Hamiltonian of the system. This causes the eigenstates to be the quasibound states which can tunnel escape out of the well within a finite time. The tunneling escape time from the double-barrier heterostructures has been measured previously by time-resolved photoluminescence experiments in the time range above 10 ps.^{12,13} It is expected, therefore, that the quasibound nature of the Stark

localized states should also be reflected in the absorption spectra line shape, especially when the barrier thickness is extremely thin and the tunneling time is short enough, due to a lifetime broadening. However, in the practical SL samples the inhomogeneous linewidth broadening prohibits observation of this effect due to the confinement potential fluctuations in the quantum-well heterostructures. Although this quasibound nature of the eigenstates has previously been discussed mostly theoretically,¹⁴⁻¹⁸ no experimental tests have been undertaken, to the best of our knowledge, for the lifetime broadening as well as the systematic dependence of the tunneling time on the barrier thickness in the time range below 10 ps.

In this paper, optical absorption spectra in two series of monolayer-controlled GaAs/AlAs SL's with ultrathin barriers have been investigated by low-temperature photocurrent spectroscopy. It is found that, when the barrier thickness in the SL samples is varied, the spectral linewidth of the fundamental Stark ladder transition under high electric fields shows systematic increases with decreasing the barrier thickness. This enhancement of the linewidth, which exceeds the inhomogeneous broadening, is due to a lifetime broadening of the quasibound Stark localized states. This resonance energy broadening due to the rapid tunneling escape of electrons is used to determine the tunneling time in the time region below 1 ps by the uncertainty principle. Good agreement is obtained between the observed tunneling time and the lifetime deduced from the calculated electron level broadening in the double-barrier QW.

In Sec. II experimental details are given, and in Sec. III results of band-edge absorption spectra and the spectral line shape analysis are first presented and discussed in Secs. III A and III B, respectively, which are followed by a discussion of the tunneling time in Sec. III C. Finally, a summary is given in Sec. IV.

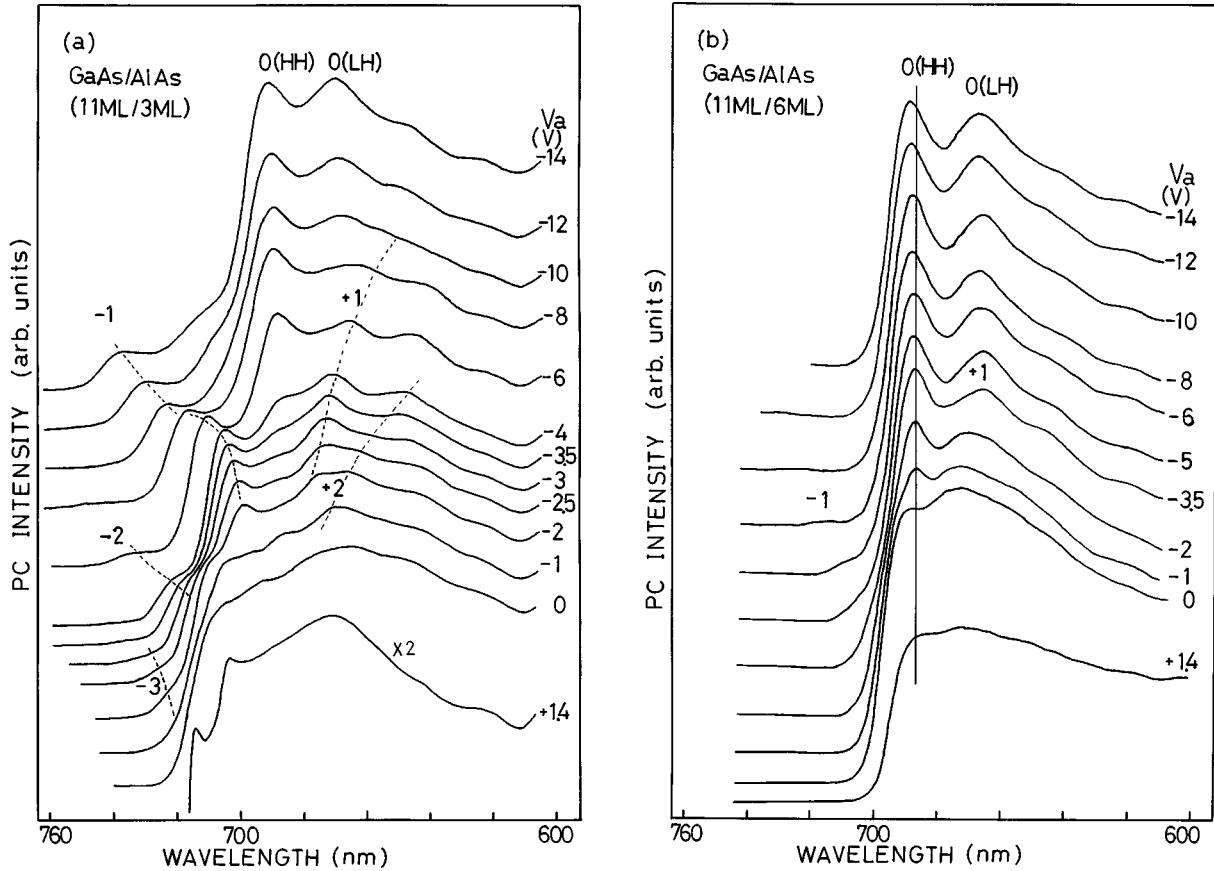


FIG. 1. Photocurrent spectra of GaAs/AlAs SL's with 11-ML GaAs wells and (a) 3-ML and (b) 6-ML AlAs barriers as a function of applied bias voltage (the minus voltage given means the reverse bias voltage). The spatially indirect heavy-hole Stark ladder transitions are denoted by ladder indices n , for example, by $+1$ and -1 , while the direct ones by $0(\text{HH})$ and $0(\text{LH})$. The spectra are vertically shifted for clarity.

II. EXPERIMENTAL DETAILS

Two different series of high-quality GaAs/AlAs SL samples were grown on GaAs(100) substrates by molecular beam epitaxy (MBE). The nominally undoped SL is contained in the intrinsic region and is sandwiched between $5 \times 10^{17} \text{ cm}^{-3}$ Si-doped $n\text{-Al}_{0.4}\text{Ga}_{0.6}\text{As}$ and 10^{18} cm^{-3} Be-doped $p\text{-Al}_{0.4}\text{Ga}_{0.6}\text{As}$ cladding layers to form a $p\text{-}i\text{-}n$ diode structure. In the first series of three SL samples, the GaAs well width L_z is fixed at 22 monolayers (ML) and the barrier thickness L_B is set at 2, 3, and 4 ML. In the second series the well width is fixed at 11 ML, while the L_B is varied from 2, 3, 4, to 6 ML. These SL samples were prepared within a short experimental period to ensure reproducibility of sample quality and uniformity. The SL period $D (=L_z+L_B)$ of some samples was measured by small-angle x-ray-diffraction experiments. These results were used to determine the actual growth rate, from which the nominal values of the well and barrier thickness were estimated within an accuracy of ± 0.1 ML. Using the simple Kronig-Penney model, miniband widths of these SL layers are calculated and the value is ranged from 14 to 144 meV for electrons. In each SL diode the 100-period SL layer is confined between undoped 50-nm $\text{Al}_{0.4}\text{Ga}_{0.6}\text{As}$ layers below and above and further n - and p -doped $\text{Al}_{0.4}\text{Ga}_{0.6}\text{As}$ cladding layers. After the growth each sample was processed into a $400 \times 400\text{-}\mu\text{m}^2$ mesa using wet chemical etching by standard photolithography techniques. A

$380 \times 380\text{-}\mu\text{m}^2$ window-shaped Au contact was then deposited onto the 10-nm p^+ -type GaAs cap layer to allow electric field application and optical access. Photocurrent (PC) spectra were measured at ~ 16 K in a closed-loop He cryostat using a halogen lamp and a monochromator for excitation and a computer-controlled electrometer for dc detection. The PC intensity was calibrated for the light intensity.

III. RESULTS AND DISCUSSION

A. PC spectral characteristics

Figures 1(a) and 1(b) show examples of PC spectra for the $L_z=11$ ML SL with $L_B=3$ and 6 ML, respectively, as a function of applied bias voltage (V_a) between $+1.4$ V (forward bias) and -14 V. At the positive bias voltage of $+1.4$ V, which nearly corresponds to the flatband condition, a sharp peak is observed at the absorption edge near 714 nm (1.737 eV) in the lowest PC spectrum in Fig. 1(a). Additionally, three peaks (one sharp and two broad features) are also seen on the high-energy side. These four features have been discussed already¹⁹ and ascribed to the heavy-hole (HH) and light-hole (LH) superlattice excitons associated with the miniband bottom (Γ) and top (Π). When the reverse bias is increased [the electric field F is given by $(V_{bi}-V_a)/W$, where V_{bi} is a built-in voltage and W the thickness of the intrinsic region], a number of new fine structures appear. On

the lower-energy side in Fig. 1(a), some peaks show redshifts, while other peaks develop at the higher-energy side (blueshifts). These evolving peaks are due to the spatially indirect Stark ladder transitions whose energies are proportional to $neFD$ with increasing the field strength F where n is a Stark ladder index.¹ Up to third order the ladder transitions can be identified. In the central region, on the other hand, two distinct peaks are gradually developing with increasing the field strength without accompanying any significant energy shifts. We attribute these peaks to the zeroth-order (fundamental) spatially direct HH and LH Stark ladder transitions.

In Fig. 1(b) are shown PC spectra for the SL sample with the relatively thick barrier thickness of 6 ML. Both direct and indirect Stark ladder transitions are also seen clearly. With increasing the reverse bias, two peaks due to the fundamental HH and LH Stark ladder transitions develop at 689 nm (1.799 eV) and 668 nm (1.856 eV). The observed energies of the leading two peaks are in agreement with calculated values of 1.777 and 1.849 eV assuming the $L_z = 11$ ML well due to HH and LH transitions, respectively. Because the SL has a narrow electron miniband of 17 meV, the Wannier-Stark localization effect is only weakly observed. However, when comparing with the two series of spectra shown in Figs. 1(a) and 1(b), we note that the linewidth of the fundamental HH transitions shows a large difference between them and that the case of thin-barrier SL is significantly broader than the thick-barrier SL. This tendency is even more pronounced for the thinnest 2-ML barrier SL.²⁰ It appears that the quantum-confined Stark effect²¹ is not important in this series of SL samples and that the peak redshift is observed to be smaller (less than 5 meV for the measured range) since the well width is narrower. If the narrow well width of 11 ML in the SL layer is taken into account, the linewidth of the zeroth-order spatially direct HH Stark ladder transition is very sharp. The linewidth of the HH fundamental Stark ladder transition is estimated by the lower half width at half maximum (HWHM) and found it to be $\sim 18.7 \pm 0.5$ meV from Fig. 1(b). This linewidth is close to a half value of ~ 29 meV calculated for the confinement energy change by one monolayer L_z fluctuations and comparable to those reported for the high-quality multiple-QW samples prepared by standard MBE technologies. Thus it is assumed that the absorption linewidth observed for the thick-barrier SL is basically determined by the inhomogeneity at the heterointerfaces (inhomogeneous broadening) as usually seen in the isolated QW. Here we only discuss the case of HH-related transitions since the LH linewidth is more difficult to evaluate due to overlapping with the HH continuum states. For the other series of SL samples with the 2 times wider wells, basically similar features were observed, although the trend is less pronounced.²²

B. Linewidth broadening

In order to show more clearly changes of the linewidth with variations of the barrier thickness, the PC spectral line shape is drawn in Fig. 2 for a set of three SL samples with $L_z = 11$ ML under the applied high electric field (reverse bias $V_a = -14$ V). For the SL sample with 4-ML barriers, additional anticrossing behaviors were observed in the PC spec-

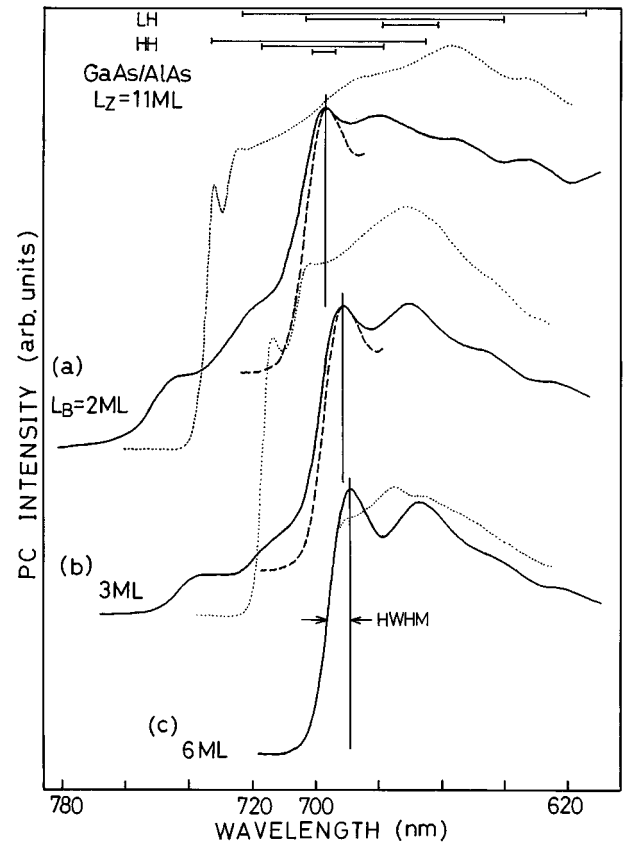


FIG. 2. Solid curves show photocurrent spectra of GaAs/AlAs SL's with 11-ML GaAs wells and (a) 2-ML, (b) 3-ML, and (c) 6-ML AlAs barriers under the applied bias voltage of -14 V, while dotted ones correspond to the flatband condition (at the forward bias voltage of $+1.4$ V). Dashed curves superimposed in (a) and (b) are the same as the spectrum (c), but shifted to align the peak position at the fundamental Stark ladder transition with keeping the base line at the height of the first-order ladder transition for comparison of the linewidth changes. Horizontal bars indicated in the upper part are the interband transition miniband widths of the superlattices related with heavy-hole (HH) and light-hole (LH) subbands. The spectra are vertically shifted for clarity.

tra. The line shape showed complicated changes with the field strength; therefore, this was omitted in Fig. 2. The PC spectra corresponding to the flatband condition are also illustrated by dotted curves. Energy positions of the miniband edge excitonic transitions are located near the wavelength regions expected from calculated transition miniband widths, also shown in the upper part of figure by horizontal bars. It is important to note that, in the voltage range where the zeroth-order Stark ladder transitions are dominating, but the Stokes shift due to the quantum-confined Stark effect (which may also contribute to the linewidth broadening) is small enough, there is a substantial difference in the linewidth between the thin- and thick-barrier SL's. In order to compare the difference in linewidth, the PC spectrum (c) for the 6-ML barrier SL is shifted and superimposed on the other spectra (a) and (b) by dashed curves in Fig. 2. In the cases (a) and (b) where the small first-order Stark ladder transition is remaining, the HWHM linewidth is estimated by shifting up the base line to the PC signal level of the first-order ladder transition. We note that in (a) and (b) the zero level of dashed spectrum coincides with the PC signal level of the first-order ladder

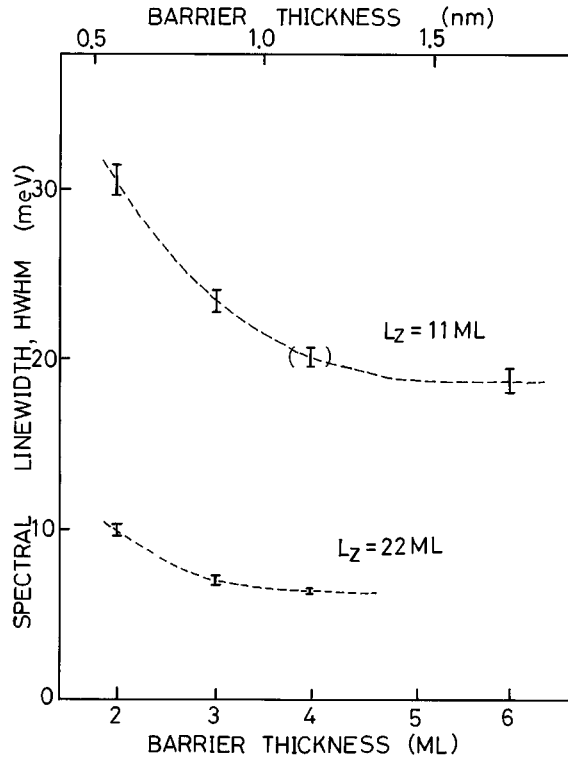


FIG. 3. Spectral linewidth (HWHM) of the zeroth-order heavy-hole Stark ladder transitions as a function of barrier thickness for the GaAs/AlAs SL with 11- and 22-ML wells. Dashed lines are guides to the eye.

transition in the solid spectra of (a) and (b). For the 2-ML (3-ML) barrier SL, a value of 30.6 ± 1 meV (23.4 ± 0.5 meV) is thus obtained for the HWHM. In Fig. 3 the experimental HWHM is plotted as a function of barrier thickness for the two series of SL samples. In the case of the $L_z = 11$ ML SL series, it is clear that the linewidth enhancement amounts to be more than 30% for the 2-ML barrier SL. It is also found that the enhancement effect is reduced when the well width becomes wider. In addition, as seen in Fig. 2, the transition peak energy of the 2-ML (3-ML) barrier SL is located by ~ 21 meV (9 meV) lower than the 6-ML barrier SL due to the reduced quantum confinement by the thinner barriers. This reduction of the confinement is also seen in the case of $L_z = 22$ ML SL's. But the reduction of the resonance energy observed with decreasing the barrier thickness is much smaller than the case of narrower well SL's, as expected, and found it to be about 5 meV when compared with 2- and 4-ML barriers. Here we assume that the experimental linewidth is determined by the sum of the homogeneous linewidth and the inhomogeneous broadening $\Gamma_h + \Gamma_{\text{inhom}}$, following von Plessen *et al.*²³ and Lee *et al.*²⁴ In the usual isolated quantum wells, the line shape of the optical transitions is practically dominated by the Γ_{inhom} and also by phonon interactions at higher temperatures.^{24,25} However, when the coherent tunneling time τ_T of the particle wave packet is extremely short for the ultrathin barriers, the $\Gamma_h (= \hbar/\tau_T)$ value due to the tunneling escape can be as large as the order of magnitude of the Γ_{inhom} . The experimental results presented in Fig. 3, especially for the thinner barrier SL, are indeed reflecting this tunneling effect, that is, the lifetime broadening. The spectral linewidth of the zeroth-order HH Stark ladder transition is actually enhanced by about 12 meV

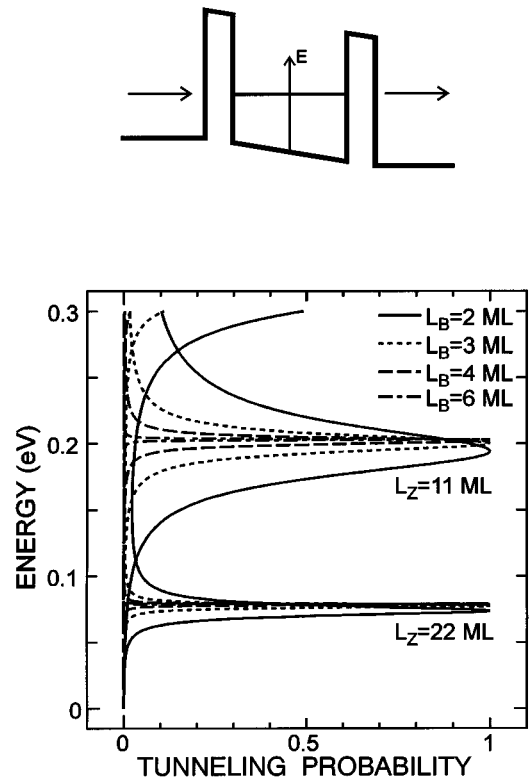


FIG. 4. Electron transmission spectra of the GaAs/AlAs double-barrier quantum-well heterostructures with 11- and 22-ML wells and different barriers between 2 and 6 ML.

(5 meV) when the barrier thickness decreases from $L_B = 6$ to 2 ML (3 ML). We note that the determination of Γ_h is based on the assumption that the different SL samples have the same value of background broadenings, assuming a constant value of 18.7 meV for the inhomogeneous broadening plus the small homogeneous broadening by phonon scattering at 16 K. These observations are consistent with our conjecture for the influences of tunneling escape time on the spectra line shape.

C. Tunneling escape time

To confirm our interpretation for the origin of the spectral linewidth enhancement when decreasing the ultrathin barrier thickness, we have performed theoretical calculations of tunneling resonances using the transfer matrix method²⁶ within the effective mass approximation. For the calculational simplicity, we have approximated the SL structure by the double barrier QW as shown in Fig. 4. This is because under the high-electric-field conditions the zeroth-order Stark ladder state is well localized in a central well and effectively confined by a pair of barriers. Furthermore, the inclined electrostatic potential under the electric field was approximated by the flat one with stair cases (0.1 nm/step) to avoid numerical complications of Airy functions. In the transmission probability calculations, the different effective masses of the particle in the well and in the barrier are accounted for and only the Γ band is considered. A conduction band offset ratio of 64/36 is assumed, and the electron effective mass ratios in the well and barriers were taken to be 0.0665 and 0.15, respectively.²⁷ Calculated results of the resonance level broadening in the conduction subband are shown in Fig. 4

for the two series of SL structures. It is found that the level broadening is very sensitive to the barrier thickness, as expected, and also depends on the well width. We have also calculated the electric field dependence on the level broadening for the model structure and found that the value is not significantly influenced, especially in the narrower well cases, for the field strength up to 300 kV/cm. For example, the calculated value of the electron tunneling resonance width ΔE_{HWHM} at $F=0$ can be as large as 23 meV for the thinnest barrier of $L_B=2$ ML when the QW width is $L_z=11$ ML. It increases slightly to 24 meV when $F=280$ kV/cm. Furthermore, when the barrier thickness L_B is decreased from 6 to 2 ML (3 ML), the calculated resonance peak energy in the conduction subband is reduced by ~ 8.7 meV (3.0 meV). This reduction of the resonance energy is in agreement with the experimental shift of 21 meV (9 meV) for the leading zeroth-order Stark ladder transition, although the calculated shifts are smaller than the experimental values. For heavy holes, on the other hand, all cases show much smaller resonance widths and smaller shifts in energy are observed with changes of the barrier thickness, and we will consider only the electron tunneling processes hereafter.

It is interesting to use the observed linewidth broadening for determining the coherent tunneling escape time $\tau_T = \hbar / \Delta E_{\text{HWHM}}$ by the uncertainty principle. We emphasize that the tunneling time discussing here through the extremely thin barriers is usually very difficult to measure directly even with using modern ultrashort optical pulse lasers due to photogenerated carrier relaxation problems.²⁸ In Fig. 5 the calculated τ_T value is shown together with the experimental values deduced from the measured linewidth enhancement. Although the theoretical values are located slightly lower than our experimental points, the barrier thickness dependence is well explained by the tunneling escape mechanism. Similar agreement between experiment and theory is also obtained for the wider SL samples with $L_z=22$ ML. In Fig. 5 the tunneling escape time measured by other groups^{12,13,29} is also included based on the different experimental methods for the relatively thicker barrier region around 2 nm. Experimental uncertainties of the time constants obtained by the optical pulse techniques are due to the radiative recombination process as well as the photogenerated charge effects. These effects might explain the reduction of measured time constants around $L_B=2.7$ nm, which are significantly deviated from our observed trend because of the stronger confinement effect. Waho *et al.*²⁹ used a completely different method from others based on the high-frequency characteristics of resonant tunneling transistors to indirectly deduce the tunneling transit time. In general, the experimental tunneling escape time and the L_B dependence are consistent with the previous results for GaAs/AlAs heterostructure systems. However, there exist some quantitative differences between them. It seems that our experimental tunneling times are systematically larger than the calculated curves. It may be related to other processes which are neglected in our simple calculations. According to recent calculations by Cabrera *et al.*,¹⁷ the tunneling escape time is significantly increased by including the carrier-phonon and electron-hole interactions, which may in part explain the quantitative disagreement.

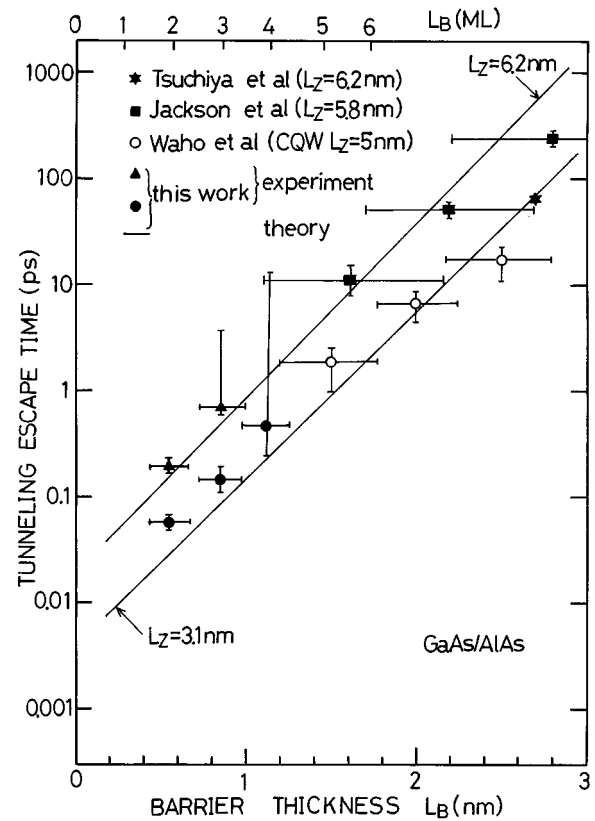


FIG. 5. Tunneling escape time from GaAs/AlAs heterostructure systems as a function of the AlAs barrier thickness.

IV. SUMMARY

Band-edge optical absorption spectra in two series of monolayer-controlled GaAs/AlAs superlattices in a p - i - n diode configuration are studied by low-temperature photocurrent spectroscopy. It is experimentally found that, in the limit of high-electric-field conditions, the linewidth of the dominating zeroth-order heavy-hole Stark ladder transition increases with systematically decreasing the barrier thickness, which exceeds the usual inhomogeneous broadening. This linewidth enhancement also depends on the well width. This enhancement effect together with the observed redshift when the barrier thickness is reduced is consistently explained by the rapid tunneling escape of electrons due to the quasibound nature of Stark localized eigenstates, i.e., by the lifetime broadening. This resonance energy broadening due to the coherent scattering by tunneling is used to determine the tunneling time by the uncertainty principle. The tunneling time thus determined and the barrier and well width dependence show good agreement with the values deduced from the confined electron level broadening for the biased double-barrier quantum-well structures based on simple transfer matrix calculations.

ACKNOWLEDGMENTS

The authors would like to thank Dr. T. Yamamoto (at present with Murata Corporation) for his expert help in the sample preparation at ATR Optical and Radio Communication Research Laboratories.

- ¹G. H. Wannier, *Rev. Mod. Phys.* **34**, 645 (1962); see also a recent review, E. E. Mendez and G. Bastard, *Phys. Today* **46** (6), 34 (1993); *Semiconductor Superlattices*, edited by H. T. Grahn (World Scientific, Singapore, 1995).
- ²J. Bleuse, G. Bastard, and P. Voisin, *Phys. Rev. Lett.* **60**, 220 (1988).
- ³E. E. Mendez, F. Agullo-Rueda, and J. M. Hong, *Phys. Rev. Lett.* **60**, 2426 (1988).
- ⁴H. Schneider, K. Kawashima, and K. Fujiwara, *Phys. Rev. B* **44**, 5943 (1991).
- ⁵M. Nakayama, I. Tanaka, H. Nishimura, K. Kawashima, and K. Fujiwara, *Phys. Rev. B* **44**, 5935 (1991).
- ⁶J. Feldmann, in *Advances in Solid State Physics*, edited by U. Rossler (Vieweg, Braunschweig, 1992), Vol. 32, p. 81.
- ⁷C. Waschke, H. Roskos, R. Schwedler, K. Leo, H. Kurz, and K. Kohler, *Phys. Rev. Lett.* **70**, 3319 (1993).
- ⁸M. Dignam, J. E. Sipe, and J. Shah, *Phys. Rev. B* **49**, 10 502 (1994).
- ⁹K. H. Schmidt, N. Linder, G. H. Dohler, H. T. Grahn, K. Ploog, and H. Schneider, *Phys. Rev. Lett.* **72**, 2769 (1994).
- ¹⁰F. Devaux, E. Bigan, M. Allovon, J. C. Harmand, F. Huet, M. Carre, and J. Landreau, *Appl. Phys. Lett.* **61**, 2773 (1992).
- ¹¹K. Kawashima, M. Hosoda, and K. Fujiwara, *Appl. Phys. Lett.* **62**, 184 (1993).
- ¹²M. Tsuchiya, T. Matsusue, and H. Sakaki, *Phys. Rev. Lett.* **59**, 2356 (1987).
- ¹³M. K. Jackson, M. B. Johnson, D. H. Chow, T. C. McGill, and C. W. Nieh, *Appl. Phys. Lett.* **54**, 552 (1989).
- ¹⁴D. Ahn and S. L. Chuang, *Phys. Rev. B* **34**, 9034 (1986).
- ¹⁵N. Harada and S. Kuroda, *Jpn. J. Appl. Phys.* **25**, 871 (1986).
- ¹⁶P. Price, *Phys. Rev. B* **38**, 1994 (1988).
- ¹⁷A. H. Cabrera, P. Aceituno, and H. Cruz, *Phys. Rev. B* **52**, 10 729 (1995).
- ¹⁸G. Gonzalez de la Cruz, I. Delgadillo, and A. Calderon, *Solid State Commun.* **98**, 357 (1996).
- ¹⁹K. Fujiwara, K. Kawashima, T. Yamamoto, N. Sano, R. Cingolani, H. T. Grahn, and K. Ploog, *Phys. Rev. B* **49**, 1809 (1994).
- ²⁰K. Kawashima, T. Yamamoto, K. Kobayashi, and K. Fujiwara, *Phys. Rev. B* **47**, 9921 (1993).
- ²¹D. A. B. Miller, D. S. Chemla, T. C. Damen, A. C. Gossard, W. Wiegmann, T. H. Wood, and C. A. Burrus, *Phys. Rev. B* **32**, 1043 (1985).
- ²²K. Fujiwara, T. Imanishi, K. Kawashima, M. Hosoda, and K. Tominaga, *Solid State Commun.* **96**, 37 (1995).
- ²³G. von Plessen, T. Meier, J. Feldmann, E. O. Gobel, P. Thomas, K. W. Goossen, J. M. Kuo, and R. F. Kopf, *Phys. Rev. B* **49**, 14 058 (1994).
- ²⁴J. Lee, E. S. Koteles, and M. O. Vassell, *Phys. Rev. B* **33**, 5512 (1986).
- ²⁵J. E. Zucker, A. Pinczuk, D. S. Chemla, and A. C. Gossard, *Phys. Rev. B* **35**, 2892 (1987).
- ²⁶P. Yuh and K. L. Wang, *Phys. Rev. B* **38**, 13 307 (1988).
- ²⁷S. Adachi, *J. Appl. Phys.* **58**, R1 (1985).
- ²⁸G. Livescu, A. M. Fox, D. A. B. Miller, T. Sizer, W. H. Knox, A. C. Gossard, and J. H. English, *Phys. Rev. Lett.* **63**, 438 (1989).
- ²⁹T. Waho, S. Koch, and T. Mizutani, *Superlatt. Microstruct.* **16**, 205 (1994).